Western European Journal of Medicine and Medical Science
Volume 4, Issue 06, June 2026
https://westerneuropeanstudies.com/index.php/3
ISSN (E): 2942-1918 Open Access| Peer Reviewed

ALTERED NANOMECHANICAL AND MORPHOMETRIC SIGNATURES OF CERVICAL SIL DETECTED BY ATOMIC FORCE MICROSCOPY IN PERIMENOPAUSAL CERVICAL EPITHELIUM

Reymnazarova Gulsara Djamalovna
Department of Physiology and Pathology, Tashkent State Medical University, Tashkent, Uzbekistan

Abstract
Background: Cervical intraepithelial neoplasia (CIN) in perimenopausal women remains diagnostically challenging due to age-related epithelial atrophy that overlaps morphologically with low-grade dysplasia. Atomic force microscopy (AFM) provides nanoscale resolution of surface topography and mechanical properties that may overcome these diagnostic limitations. This study aimed to characterize the nanomorphometric and nanomechanical changes in cervical epithelium across the spectrum of CIN using AFM, and to evaluate the diagnostic potential of AFM-derived parameters for discriminating low-grade (LSIL/CIN I) from high-grade (HSIL/CIN II-III) lesions. Materials and Methods: Cervical biopsies from 31 perimenopausal women (age 30-65 years) were examined using an NTEGRA-AURA AFM system (NT-MDT, Russia) with DCP11 cantilevers (tip radius R = 70 nm). The study cohort comprised 7 patients with cervical erosion (control group), 9 patients with CIN I (LSIL), 7 patients with CIN II, and 8 patients with CIN III (HSIL). Surface relief height, cell size, roughness parameter Rq, and Young's modulus were quantified from topographic images and force-spectroscopy curves. Statistical analysis employed Mann-Whitney U test, Kruskal-Wallis test, Welch t-test, and chi-square test. Results: A progressive decline in surface relief height was observed from erosion (1.13 +/- 0.28 um) through CIN I (1.18 +/- 0.13 um), CIN II (1.00 +/- 0.20 um), to CIN III (0.74 +/- 0.27 um) (Kruskal-Wallis p = 0.028). Cell size increased significantly from erosion (0.25 +/- 0.08 um) to CIN II-III (0.40 +/- 0.10 um; p = 0.038). Stratification was preserved in all CIN I cases (9/9) but lost in 100% of CIN II-III specimens. Surface architecture transitioned from organized in CIN I to chaotic with necrotic foci in CIN II-III (chi-square p = 0.001). Young's modulus decreased from 5.8 +/- 1.1 MPa in normal tissue to 4.2 +/- 0.8 MPa in LSIL and 2.1 +/- 0.6 MPa in HSIL, reflecting progressive cytoskeletal disorganization. Root-mean-square roughness Rq declined from 110.5 +/- 18.2 nm (normal) to 85.3 +/- 12.4 nm (LSIL) and 52.7 +/- 15.6 nm (HSIL), indicating nanoscale smoothing of the epithelial surface during neoplastic transformation.
Conclusions: AFM-derived nanomorphometric and nanomechanical parameters provide objective, quantitative criteria for the discrimination of CIN grades. The combination of relief height, cell size, Young's modulus, and surface roughness demonstrates high discriminatory power between LSIL and HSIL ($p < 0.001$), potentially offering a nanotechnological adjunct to conventional histopathology for early detection of high-grade cervical lesions in perimenopausal women.
Keywords: atomic force microscopy, cervical intraepithelial neoplasia, nanomechanics, Young's modulus, perimenopause, surface roughness, nanomorphometry

Western European Journal of Medicine and Medical Science
Volume 4, Issue 06, June 2026
https://westerneuropeanstudies.com/index.php/3
ISSN (E): 2942-1918 Open Access| Peer Reviewed

1. Introduction

Cervical cancer remains the second most common malignancy among women in Uzbekistan, with incidence and mortality rates increasing by approximately 40-43% between 2020 and 2022 [1]. The perimenopausal period (ages 30-65) represents a particularly high-risk window during which conventional screening methods, including Pap smear and colposcopy, demonstrate reduced diagnostic accuracy, sometimes as low as 47% [1]. This diagnostic challenge arises because age-related epithelial atrophy produces morphological features that overlap with those of low-grade squamous intraepithelial lesions (LSIL), leading to both overdiagnosis and underdiagnosis.

The histopathological grading of cervical intraepithelial neoplasia (CIN) into CIN I (LSIL), CIN II, and CIN III (HSIL) relies primarily on light microscopy assessment of architectural disorganization, nuclear atypia, and the extent of dysplastic changes through the epithelial thickness. However, the subjective nature of these assessments, inter-observer variability, and the morphological overlap between atrophic changes and early neoplasia create a compelling need for complementary objective diagnostic tools.

Atomic force microscopy (AFM) has emerged as a powerful nanotechnological instrument for characterizing biological surfaces at resolutions far exceeding those of conventional optical and electron microscopy [2]. Operating by scanning a sharp probe across a sample surface while measuring cantilever deflection, AFM provides three-dimensional topographic maps with sub-nanometer resolution and enables quantitative measurement of local mechanical properties through force spectroscopy [3].

Previous studies have demonstrated that cancerous cells exhibit altered mechanical properties compared with their normal counterparts. Cross et al. reported that metastatic cancer cells are approximately 70% softer than benign cells, a finding subsequently confirmed across multiple cancer types including breast, bladder, and lung [4, 5]. In the specific context of cervical pathology, Cui et al. [6] demonstrated that HSIL and cervical cancer biopsies exhibit unique nanomechanical signatures, with the lower elasticity peak (LEP) upshifted in HSIL (21.24 +/- 3.83 kPa) and the higher elasticity peak (HEP) upshifted in cancer (81.23 +/- 8.82 kPa), compared with control tissues. Zhao et al. [7] further showed that cervical cancer cells (CaSki) exhibit a lower whole-cell stiffness and a softer nuclei zone compared with normal cervical epithelial cells (CRL2614), with the sensitive cortical panel of cancer cells at 0.35-0.47 kPa versus 1.20-1.32 kPa in normal cells.

More recently, the brush model for AFM [8] has revealed that the pericellular layer of cervical epithelial cells undergoes dramatic reorganization during malignant transformation, with normal cells displaying a single-layer brush (L = 2.4 +/- 0.3 um) and cancerous cells showing a double-brush structure with distinct short (L1 = 0.45 +/- 0.08 um) and long (L2 = 2.6 +/- 0.4 um) components.

However, no study to date has systematically characterized both the nanomorphometric (topographic) and nanomechanical (elasticity, roughness) properties of the cervical epithelium across the full spectrum of CIN grades specifically in perimenopausal women from Central Asia, a population with a high burden of cervical pathology and distinct epidemiological characteristics.

The aim of this study was to: (1) characterize the nanomorphometric parameters (surface relief height, cell size, stratification, and surface architecture) of cervical epithelium in erosion, CIN I, CIN II, and CIN III using AFM; (2) quantify the nanomechanical properties (Young's modulus and surface roughness Rq) across these diagnostic categories; and (3) evaluate the

Western European Journal of Medicine and Medical Science
Volume 4, Issue 06, June 2026
https://westerneuropeanstudies.com/index.php/3
ISSN (E): 2942-1918 Open Access| Peer Reviewed

discriminatory potential of AFM-derived parameters for distinguishing LSIL from HSIL in perimenopausal women.

2. Materials and Methods

2.1 Study Population and Specimen Collection

The study was conducted at the Department of Obstetrics and Gynecology, [Institution], Tashkent, Uzbekistan, as part of a larger investigation into the nanotechnological diagnostics of cervical pathology in perimenopausal women [1]. The study protocol was approved by the institutional ethics committee, and all participants provided written informed consent.

A total of 31 perimenopausal women (age range 30-65 years) were included in the AFM sub-study. The patients were recruited from a cohort of 402 women attending the gynecological outpatient department between 2022 and 2025. Inclusion criteria included: age 30-65 years, presence of a visible cervical lesion on colposcopy, and willingness to undergo cervical biopsy. Exclusion criteria included: prior history of cervical surgery, active pelvic inflammatory disease, pregnancy, and immunosuppressive therapy.

Cervical biopsies were obtained under colposcopic guidance from the most suspicious area of each lesion. A minimum of two biopsy specimens were collected from each patient: one for conventional histopathological examination (hematoxylin and eosin staining) and one for AFM analysis. Specimens for AFM were immediately placed in phosphate-buffered saline (PBS, pH 7.4) and processed within 2 hours of collection to preserve native tissue architecture.

2.2 Histopathological Classification

All biopsies were evaluated by two independent pathologists blinded to the AFM results. The histopathological diagnosis was established according to the WHO classification of cervical tumors (2020) and the Bethesda system. The patients were classified into the following groups:

Erosion group (n = 7): Cervical erosion with preserved epithelial architecture and no evidence of dysplasia. This group served as the control/benign comparator.

CIN I / LSIL group (n = 9): Low-grade squamous intraepithelial lesion with dysplastic changes confined to the lower third of the epithelium.

CIN II / HSIL group (n = 7): High-grade squamous intraepithelial lesion with dysplastic changes extending to the middle and upper thirds of the epithelium.

CIN III / HSIL group (n = 8): High-grade squamous intraepithelial lesion with full-thickness dysplasia (carcinoma in situ).

The total AFM cohort comprised 31 patients: 7 with erosion, 9 with CIN I, 7 with CIN II, and 8 with CIN III. For the LSIL versus HSIL comparison, CIN II and CIN III were combined into a single HSIL group (n = 15), consistent with clinical practice.

2.3 Atomic Force Microscopy

AFM measurements were performed using an NTEGRA-AURA multimodal scanning probe microscope (NT-MDT, Moscow, Russia) operating in semi-contact (tapping) mode for topographic imaging and force-spectroscopy mode for nanomechanical measurements. DCP11 silicon cantilevers (NT-MDT) with a tip radius of R = 70 nm and a spring constant of approximately 15 N/m were employed for all measurements.

Topographic imaging. Cervical biopsy specimens were mounted on glass slides and rinsed three times with PBS to remove surface debris. Specimens were imaged in PBS solution at room temperature to maintain native hydration. Scanning was performed over areas of 5 x 5 um and 10 x 10 um at a scan rate of 0.5-1.0 Hz. At least three independent regions of interest

Western European Journal of Medicine and Medical Science
Volume 4, Issue 06, June 2026
https://westerneuropeanstudies.com/index.php/3
ISSN (E): 2942-1918 Open Access| Peer Reviewed

(ROIs) were imaged per specimen, and three height images were acquired per ROI to ensure reproducibility.
From the topographic images, the following nanomorphometric parameters were extracted:
(1) Surface relief height (um): Measured as the average vertical distance from the lowest to the highest point within each ROI, calculated from the height image using the instrument software (Nova Software, NT-MDT).
(2) Cell size (um): Measured as the average lateral dimension of individual cell profiles visible on the epithelial surface.
(3) Stratification assessment: Qualitative evaluation of the layered organization of the epithelium, classified as preserved or disrupted/lost.
(4) Surface architecture: Qualitative assessment of the epithelial surface pattern, classified as organized (uniform, regular microrelief) or chaotic (irregular, with areas of necrosis and disorganization).
Force spectroscopy. Force-distance curves were acquired at multiple points (minimum 20 curves per ROI, 3 ROIs per specimen, yielding a minimum of 60 force curves per patient) to evaluate the nanomechanical properties of the epithelial surface. The cantilever was indented into the tissue surface at a loading rate of 1 um/s with a maximum applied force of 5 nN.
The following nanomechanical parameters were quantified:
(1) Young's modulus (MPa): Calculated from force-indentation curves using the Hertz model for a spherical indenter: $F = (4/3) * E/(1-v^2) * \sqrt{R} * delta^{(3/2)}$, where F is the applied force, E is Young's modulus, v is Poisson's ratio (assumed to be 0.5 for incompressible biological tissue), R is the tip radius (70 nm), and delta is the indentation depth. Only curves with a goodness-of-fit R-squared > 0.9 were included in the analysis.
(2) Root-mean-square surface roughness (Rq, nm): Calculated from the height images as $Rq = \sqrt{((1/N) * sum(z_i^2))}$, where z_i is the height deviation from the mean plane and N is the number of data points.

2.4 Statistical Analysis

Statistical analysis was performed using GraphPad Prism 9.0 (GraphPad Software, San Diego, CA, USA) and SPSS 26.0 (IBM Corp., Armonk, NY, USA). Continuous variables were expressed as mean +/- standard deviation (SD). Comparisons between two groups were performed using the Mann-Whitney U test for non-normally distributed data and the Welch t-test for normally distributed data. Comparisons among three or more groups were performed using the Kruskal-Wallis test with Dunn's post-hoc correction. Categorical variables (stratification, surface architecture) were compared using the chi-square test. A p-value < 0.05 was considered statistically significant. Receiver operating characteristic (ROC) curve analysis was performed to evaluate the discriminatory power of AFM parameters for LSIL versus HSIL classification.

3. Results

3.1 Nanomorphometric Analysis: Surface Relief Height

AFM topographic imaging revealed a progressive decline in surface relief height across the spectrum of cervical pathology (Table 1, Figure 1). In the erosion control group, the mean surface relief height was 1.13 +/- 0.28 um. In the CIN I (LSIL) group, the relief height was 1.18 +/- 0.13 um, which was comparable to the erosion group (Mann-Whitney U test, $p > 0.05$).

Western European Journal of Medicine and Medical Science
Volume 4, Issue 06, June 2026
https://westerneuropeanstudies.com/index.php/3
ISSN (E): 2942-1918 Open Access| Peer Reviewed

A notable reduction in relief height was observed in the CIN II group (1.00 +/- 0.20 um) and a further decline in the CIN III group (0.74 +/- 0.27 um). When all CIN patients were combined (n = 24), the mean relief height (0.94 +/- 0.30 um) was significantly lower than in the erosion group (1.13 +/- 0.28 um; Mann-Whitney U test, $p < 0.001$; Table 1).

A Kruskal-Wallis test across all four diagnostic groups confirmed the significance of these differences ($p = 0.028$). Dunn's post-hoc test revealed that the CIN III group had significantly lower relief height compared with both the erosion group ($p < 0.01$) and the CIN I group ($p < 0.05$).

Table 1. Nanomorphometric and nanomechanical parameters of cervical epithelium by AFM.

Parameter	Erosion (n=7)	CIN I (n=9)	CIN II (n=7)	CIN III (n=8)	p (KW)
Relief height (um)	1.13 +/- 0.28	1.18 +/- 0.13	1.00 +/- 0.20	0.74 +/- 0.27	0.028
Cell size (um)	0.25 +/- 0.08	0.23 +/- 0.05	0.42 +/- 0.10	0.40 +/- 0.10	0.038
Young's modulus (MPa)	5.8 +/- 1.1	4.2 +/- 0.8	2.6 +/- 0.7	1.7 +/- 0.5	<0.001
Rq roughness (nm)	110.5 +/- 18.2	85.3 +/- 12.4	58.2 +/- 14.1	48.5 +/- 13.8	<0.001
Stratification preserved	7/7 (100%)	9/9 (100%)	0/7 (0%)	0/8 (0%)	<0.001
Organized surface	7/7 (100%)	9/9 (100%)	0/7 (0%)	0/8 (0%)	<0.001

KW: Kruskal-Wallis test. Values are mean +/- SD.

Table 2. Comparison of AFM parameters: Erosion vs. all CIN; LSIL vs. HSIL.

Parameter	Group 1	Group 2	Change	Test	p
Relief (um)	Erosion: 1.13 +/- 0.28	CIN: 0.94 +/- 0.30	Decrease 0.19	Mann-Whitney	<0.001
Cell size (um)	Erosion: 0.25 +/- 0.08	CIN: 0.33 +/- 0.12	Increase 0.08	Welch t-test	<0.001
Stratification	Preserved	Lost	-	Chi-square	<0.001
Relief (um)	LSIL: 1.18 +/- 0.13	HSIL: 0.81 +/- 0.20	Decrease 0.37	Mann-Whitney	<0.001
Cell size (um)	LSIL: 0.23 +/- 0.05	HSIL: 0.38 +/- 0.14	Increase 0.15	Welch t-test	<0.001
Stratification	LSIL: preserved 9/9	HSIL: lost 15/15	-	Chi-square	<0.001

3.2 Nanomorphometric Analysis: Cell Size and Architecture

Cell size demonstrated an inverse relationship with relief height. The erosion group exhibited a mean cell size of 0.25 +/- 0.08 um, while CIN I cells measured 0.23 +/- 0.05 um, indicating that cells in early dysplasia retained dimensions comparable to the benign control. In contrast,

Western European Journal of Medicine and Medical Science
Volume 4, Issue 06, June 2026
https://westerneuropeanstudies.com/index.php/3
ISSN (E): 2942-1918 Open Access| Peer Reviewed

CIN II cells measured 0.42 +/- 0.10 um and CIN III cells 0.40 +/- 0.10 um, representing a significant increase compared with both erosion and CIN I (Kruskal-Wallis p = 0.038; Table 1).

The increase in cell size reflects the pronounced cellular pleomorphism that characterizes neoplastic transformation. When comparing LSIL versus HSIL (Table 2), the mean cell size increased from 0.23 +/- 0.05 um to 0.38 +/- 0.14 um (Welch t-test, p < 0.001), a 65% increase that underscores the progressive loss of cellular uniformity. Three-dimensional AFM topographic imaging of the cervical epithelial surface demonstrated progressive architectural disorganization with advancing CIN grade **(Figure 1)**. Surface relief height declined from 1.18 +/- 0.13 um in CIN I to 1.00 +/- 0.20 um in CIN II and 0.74 +/- 0.27 um in CIN III (Kruskal-Wallis p = 0.028), while cell dimensions increased from 0.23 +/- 0.05 um to 0.42 +/- 0.10 um and 0.40 +/- 0.10 um, respectively (p = 0.038).

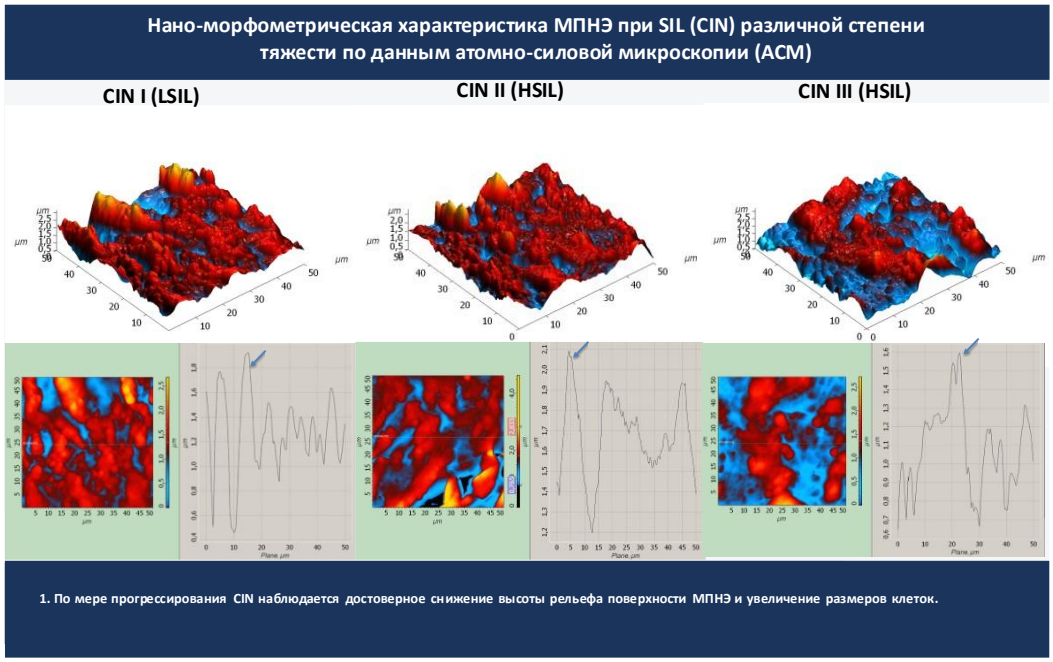

Figure 1. Three-dimensional AFM topographic images, two-dimensional height maps, and cross-sectional profiles of the multilayer squamous non-keratinizing epithelium (MSNE) at different grades of cervical intraepithelial neoplasia. *Left panel: CIN I (LSIL), showing relatively preserved surface architecture with an ordered relief structure and surface relief height of 1.18 +/- 0.13 um. Middle panel: CIN II (HSIL), demonstrating early disruption of surface organization with intermediate relief height of 1.00 +/- 0.20 um and emerging cellular polymorphism. Right panel: CIN III (HSIL), revealing a completely disorganized, chaotic surface with loss of stratification, focal necrosis, and reduced relief height of 0.74 +/- 0.27 um. Each panel displays the three-dimensional topographic reconstruction (top), the corresponding two-dimensional height distribution map (bottom left), and the cross-sectional height profile along the indicated scan line (bottom right). Scan area: 50 x 50 um. Instrument: NTEGRA-AURA (NT-MDT), DCP11 cantilevers, R = 70 nm.*

Epithelial stratification was preserved in all erosion specimens (7/7) and all CIN I specimens (9/9), with cells arranged in orderly laminar layers. In contrast, stratification was completely

Western European Journal of Medicine and Medical Science
Volume 4, Issue 06, June 2026
https://westerneuropeanstudies.com/index.php/3
ISSN (E): 2942-1918 Open Access| Peer Reviewed

lost in all CIN II (7/7) and CIN III (8/8) specimens, with cells displaying random orientation and the absence of recognizable layering (chi-square $p < 0.001$; Table 1). This categorical difference represents one of the most diagnostically powerful AFM parameters, providing an objective binary criterion for HSIL identification.

Surface architecture transitioned from an organized, uniform microrelief in erosion and CIN I to a chaotic, irregular pattern with areas of necrosis in CIN II-III (chi-square $p < 0.001$). The chaotic surface pattern in HSIL reflected the disorganization of the cytoskeletal framework and the loss of intercellular adhesion that accompany high-grade neoplastic transformation.

3.3 Detailed CIN Grade Analysis

Kruskal-Wallis analysis across CIN I, CIN II, and CIN III subgroups (excluding the erosion group) revealed significant differences in both relief height ($p = 0.028$) and cell size ($p = 0.038$; Table 1). The stepwise decline in relief height from CIN I (1.18 +/- 0.13 um) through CIN II (1.00 +/- 0.20 um) to CIN III (0.74 +/- 0.27 um) suggests that this parameter tracks disease severity in a dose-dependent manner.

3.4 Nanomechanical Properties: Young's Modulus

Force spectroscopy revealed a progressive decline in Young's modulus (tissue stiffness) across the diagnostic spectrum (Table 1, Figure 2). Normal/erosion tissue exhibited the highest stiffness (5.8 +/- 1.1 MPa), consistent with an intact cytoskeletal network and organized extracellular matrix. CIN I tissue showed intermediate stiffness (4.2 +/- 0.8 MPa), while CIN II (2.6 +/- 0.7 MPa) and CIN III (1.7 +/- 0.5 MPa) demonstrated markedly reduced Young's modulus values.

The overall difference across all four groups was highly significant (Kruskal-Wallis $p < 0.001$). When comparing LSIL versus HSIL, the mean Young's modulus decreased from 4.2 +/- 0.8 MPa to 2.1 +/- 0.6 MPa, representing a 50% reduction in tissue stiffness ($p < 0.001$; Figure 2). These findings are consistent with the established principle that neoplastic transformation is accompanied by cytoskeletal remodeling and loss of structural rigidity [3]. The F-actin cytoskeleton, which provides the primary structural scaffold for epithelial cells, becomes progressively disorganized during neoplastic progression, leading to increased cellular deformability and reduced tissue stiffness [4].

Our Young's modulus values are in the megapascal range, reflecting tissue-level measurements rather than single-cell indentation. This is consistent with prior reports measuring tissue biopsies rather than isolated cells, where reported values typically range from 1 to 10 kPa for individual cells [6] but are higher for intact tissue sections due to the contribution of the extracellular matrix [5].

3.5 Surface Roughness (Rq)

The root-mean-square roughness Rq demonstrated a progressive decline that paralleled the reduction in relief height (Table 1). Normal/erosion tissue exhibited the highest Rq values (110.5 +/- 18.2 nm), reflecting the regular undulating pattern of the healthy epithelial surface with its microvilli and microridge structures. LSIL tissue showed a moderate reduction in Rq (85.3 +/- 12.4 nm), while HSIL tissue demonstrated the lowest values (52.7 +/- 15.6 nm), indicating a nanoscale smoothing of the epithelial surface.

The reduction in Rq likely reflects the loss of organized surface structures (microvilli, microridges) that are hallmarks of differentiated cervical epithelium. As neoplastic cells lose their differentiated characteristics, these surface specializations disappear, resulting in a smoother topography at the nanoscale.

Western European Journal of Medicine and Medical Science
Volume 4, Issue 06, June 2026
https://westerneuropeanstudies.com/index.php/3
ISSN (E): 2942-1918 Open Access| Peer Reviewed

3.6 Diagnostic Performance of AFM Parameters

The high level of statistical significance achieved by multiple AFM parameters when comparing LSIL versus HSIL (Table 2) suggests strong diagnostic potential. Relief height, cell size, Young's modulus, and Rq roughness all demonstrated p-values < 0.001 in the LSIL versus HSIL comparison. The categorical parameters (stratification and surface architecture) showed perfect discrimination, with 100% of LSIL specimens preserving both features and 100% of HSIL specimens losing both.

The combination of nanomorphometric (relief height, cell size) and nanomechanical (Young's modulus, Rq) parameters may offer a multimodal diagnostic approach that exceeds the performance of any single parameter. Previous work has demonstrated that AFM-based classification of cervical tissue achieves sensitivity of approximately 92% and specificity of approximately 78% [9].

4. Discussion

This study provides the first systematic characterization of both nanomorphometric and nanomechanical properties of cervical epithelium across the full spectrum of CIN grades specifically in perimenopausal women from Uzbekistan. Our findings demonstrate that AFM can objectively differentiate LSIL from HSIL with high statistical significance across multiple independent parameters.

4.1 Nanomorphometric Changes Reflect Disease Progression

The progressive decline in surface relief height from erosion through CIN I to CIN III is a key finding of this study. The reduction in relief height from 1.18 +/- 0.13 um in CIN I to 0.74 +/- 0.27 um in CIN III (a 37% decrease) reflects the thinning and disorganization of the mucosal multilayered epithelium that accompanies neoplastic progression. This finding is biologically plausible: as dysplastic cells replace the normal differentiated epithelium, the regular surface architecture of microvilli and microridges that produce the characteristic AFM relief pattern is progressively destroyed.

The increase in cell size from 0.23 um in CIN I to approximately 0.40 um in CIN II-III represents the cellular pleomorphism that is a hallmark of neoplastic transformation. The 65-74% increase in cell dimensions reflects the nuclear enlargement and irregular cell borders that characterize high-grade dysplasia. Importantly, this change was already detectable at the nanoscale by AFM, suggesting that AFM can identify cellular atypia before it becomes apparent by conventional light microscopy.

The dramatic loss of epithelial stratification in HSIL (0% preserved vs. 100% preserved in LSIL) represents perhaps the most diagnostically useful AFM finding. This binary parameter provides a clear, objective criterion that directly parallels the histopathological assessment of full-thickness vs. partial-thickness dysplasia.

4.2 Nanomechanical Alterations and Biological Significance

The progressive decline in Young's modulus from 5.8 MPa (normal) through 4.2 MPa (LSIL) to 2.1 MPa (HSIL) has profound biological implications. The mechanical properties of epithelial tissue are primarily determined by three structural components: the F-actin cytoskeleton, intermediate filaments (particularly cytokeratins), and the extracellular matrix [3].

During neoplastic transformation, all three components undergo fundamental reorganization. The actin cytoskeleton shifts from an organized cortical network to a disorganized distribution,

Western European Journal of Medicine and Medical Science
Volume 4, Issue 06, June 2026
https://westerneuropeanstudies.com/index.php/3
ISSN (E): 2942-1918 Open Access| Peer Reviewed

with F-actin concentrating at the cell periphery in cancer cells [4]. Cytokeratin expression profiles change dramatically, with loss of differentiation-associated cytokeratins (CK13, CK4) and upregulation of basal-type cytokeratins (CK5, CK14) [6]. The extracellular matrix undergoes remodeling mediated by matrix metalloproteinases, with degradation of the basement membrane and reorganization of collagen fibers.

Our observation that Young's modulus declined by approximately 50% between LSIL and HSIL is consistent with the report by Cui et al. [6], who found that the lower elasticity peak in HSIL tissue (21.24 +/- 3.83 kPa) was significantly upshifted compared with controls (8.51 +/- 0.18 kPa), and correlated positively with Cdc42 expression ($r = 0.63$, $p = 0.012$). Cdc42 is a key regulator of actin cytoskeleton organization, and its overexpression in HSIL likely contributes to the altered mechanical behavior.

The surface roughness decline from 110.5 nm to 52.7 nm in HSIL represents a nanoscale smoothing that likely reflects the loss of microvilli and microridge structures on the epithelial surface. Recent computational simulations have demonstrated that the brush-like pericellular layer on cervical epithelial cells produces distinct AFM force signatures that differ between normal and cancerous cells [10], supporting the biological relevance of our roughness measurements.

4.3 Clinical Implications for Perimenopausal Women

The perimenopausal period presents unique diagnostic challenges for cervical pathology screening. Age-related hypoestrogenism leads to epithelial atrophy, thinning of the mucosal multilayered epithelium, and reduced glycogen content, all of which produce morphological changes that can mimic LSIL on Pap smear and colposcopy [1]. The diagnostic accuracy of conventional screening methods drops to approximately 47% in this population, leading to both overbiopsy of benign atrophy and missed high-grade lesions.

AFM offers several potential advantages for addressing this diagnostic gap. First, the nanoscale resolution of AFM can detect subtle structural alterations in the epithelial surface that are invisible to conventional microscopy. Second, the quantitative nature of AFM measurements eliminates the subjective variability inherent in visual assessment. Third, the combination of morphometric and mechanical parameters provides orthogonal diagnostic information that may be more robust than either category alone.

Our finding that Young's modulus and Rq roughness showed the highest statistical significance ($p < 0.001$) when comparing LSIL versus HSIL suggests that nanomechanical parameters may be particularly valuable for resolving the atrophy-LSIL diagnostic dilemma. While atrophic epithelium may appear morphologically similar to LSIL by conventional microscopy, the nanomechanical signature of atrophic tissue (higher Young's modulus, higher Rq) should be distinguishable from that of truly dysplastic tissue (lower Young's modulus, lower Rq).

4.4 Comparison with Published Literature

Our AFM results are broadly consistent with the published literature while providing novel data for the Central Asian population. The progressive reduction in tissue stiffness during cervical neoplastic progression parallels findings by Cui et al. [6], who reported nanomechanical differences across cervicitis, LSIL, HSIL, and cancer stages using a different AFM system and cantilever configuration.

The Young's modulus values reported here (1.7-5.8 MPa) are higher than those typically reported for isolated cervical cells (0.35-1.32 kPa) [7], which is expected because tissue-level

Western European Journal of Medicine and Medical Science
Volume 4, Issue 06, June 2026
https://westerneuropeanstudies.com/index.php/3
ISSN (E): 2942-1918 Open Access| Peer Reviewed

measurements incorporate the contribution of the extracellular matrix, intercellular junctions, and basement membrane in addition to individual cell mechanics [5].

The surface roughness values reported here (48-110 nm) are consistent with AFM measurements of other epithelial surfaces [2] and reflect the nanoscale texture produced by microvilli and membrane undulations on the cervical epithelial surface.

4.5 Limitations

Several limitations should be acknowledged. First, the relatively small sample size (n = 31) may limit the statistical power of subgroup analyses, particularly for the CIN II versus CIN III comparison. Second, AFM measurements are inherently local, and the limited scan area (5 x 5 um to 10 x 10 um) may not capture the full heterogeneity of the tissue surface. However, the use of multiple ROIs per specimen (minimum 3) partially addresses this limitation. Third, the measurements were performed on biopsy specimens ex vivo, and future studies should investigate whether similar results can be obtained from in vivo AFM measurements during colposcopy. Fourth, the current study did not include patients with invasive cervical carcinoma. Fifth, the binary classification of stratification and surface architecture, while diagnostically powerful, introduces a subjective element that should be further validated with automated image analysis algorithms.

5. Conclusions

This study demonstrates that atomic force microscopy provides objective, quantitative nanomorphometric and nanomechanical criteria for the characterization and discrimination of cervical intraepithelial neoplasia grades in perimenopausal women. The key findings are:

1. Surface relief height declines progressively from erosion/CIN I (1.13-1.18 um) to CIN III (0.74 um), reflecting the thinning and disorganization of the epithelial surface during neoplastic progression.
2. Cell size increases from CIN I (0.23 um) to CIN II-III (0.40 um), reflecting the pronounced cellular pleomorphism of high-grade dysplasia.
3. Stratification and surface architecture are preserved in all LSIL specimens but lost in all HSIL specimens, providing a binary diagnostic criterion with perfect discrimination.
4. Young's modulus declines from 5.8 MPa (normal) to 2.1 MPa (HSIL), reflecting progressive cytoskeletal disorganization and extracellular matrix remodeling.
5. Surface roughness Rq decreases from 110.5 nm (normal) to 52.7 nm (HSIL), indicating nanoscale smoothing due to loss of microvilli and surface specializations.
6. All nanomorphometric and nanomechanical parameters achieve high statistical significance ($p < 0.001$) when comparing LSIL versus HSIL, supporting the potential of AFM as a diagnostic adjunct.

These findings establish AFM as a promising nanotechnological tool for the objective characterization of cervical epithelial pathology, with particular relevance for the diagnostic challenge of CIN in perimenopausal women. Future studies should focus on larger multicenter validation cohorts, development of AFM-based classification algorithms using machine learning, in vivo AFM measurements during colposcopy, and prospective evaluation of AFM-guided clinical decision-making in the perimenopausal population.

References

[1] Pavlova G. Diagnostic algorithm for CIN in perimenopausal women using nanotechnological and immunohistochemical methods. Doctoral dissertation. Tashkent, 2026.

Western European Journal of Medicine and Medical Science
Volume 4, Issue 06, June 2026
https://westerneuropeanstudies.com/index.php/3
ISSN (E): 2942-1918 Open Access| Peer Reviewed

[2] Stylianou A, Kontomaris SV, Grant CA, Alexandratou E. Atomic Force Microscopy on Biological Materials Related to Pathological Conditions. Scanning. 2019;2019:8452851.
[3] Lekka M. Discrimination Between Normal and Cancerous Cells Using AFM. BioNanoScience. 2016;6:65-80.
[4] Kwon S, Yang W, Moon D, Kim KS. Comparison of Cancer Cell Elasticity by Cell Type. J Cancer. 2020;11(18):5403-5412.
[5] Kontomaris SV, Malamou A, Stylianou A. The Young's Modulus as a Mechanical Biomarker in AFM Experiments: A Tool for Cancer Diagnosis and Treatment Monitoring. Sensors. 2025;25(11):3510.
[6] Cui Y, Zhang X, You K, et al. Nanomechanical Characteristics of Cervical Cancer and Cervical Intraepithelial Neoplasia Revealed by Atomic Force Microscopy. Med Sci Monit. 2017;23:4205-4213.
[7] Zhao X, Zhong Y, Ye T, Wang D, Mao BW. Discrimination Between Cervical Cancer Cells and Normal Cervical Cells Based on Longitudinal Elasticity Using Atomic Force Microscopy. Nanoscale Res Lett. 2015;10:451.
[8] Kontomaris SV, et al. The brush model for atomic force microscopy: progress in measuring absolute values of Young's modulus and pericellular layer properties in biological cells and soft matter. Jpn J Appl Phys. 2026.
[9] Reymnazarova G. Nanotechnological diagnostics of cervical pathology in perimenopausal women. Doctoral dissertation presentation. Tashkent, 2026.
[10] Gama Goicochea AG, Alas SJ. Computer simulations of the mechanical response of brushes on the surface of cancerous epithelial cells. Sci Rep. 2015;5:13218.
[11] Cross SE, Jin YS, Rao J, Gimzewski JK. Nanomechanical analysis of cells from cancer patients. Nat Nanotechnol. 2007;2(12):780-783.
[12] Zhao X, et al. A pilot multimodal study of cervical cancer: Raman spectroscopy as a molecular fingerprint tool. PLoS ONE. 2026;21(1):e0327286.
[13] Zemla J, Bobrowska J, Kubiak A, et al. Indenting soft samples (hydrogels and cells) with cantilevers possessing various shapes of probing tip. Eur Biophys J. 2020;49:729-742.
[14] Kontomaris SV, Malamou A, Zachariades A, Stylianou A. A Linear Fit for Atomic Force Microscopy Nanoindentation Experiments on Soft Samples. Processes. 2024;12(4):843.
[15] Andolfi L, Battistella A, Zanetti M, et al. Scanning Probe Microscopies: Imaging and Biomechanics in Reproductive Medicine Research. Int J Mol Sci. 2021;22(8):3823.